Biogeosciences Discuss., doi:10.5194/bg-2016-261, 2016
Manuscript under review for journal Biogeosciences
Published: 6 September 2016
© Author(s) 2016. CC-BY 3.0 License.

Biogeosciences Discussions
Open Access
EGU

Long-term Carbon and Nitrogen Dynamics at SPRUCE Revealed through Stable Isotopes in Peat Profiles

Erik A. Hobbie[1], Janet Chen[1,2], Paul J. Hanson[3], Colleen M. Iversen[3], Karis J. Mcfarlane[4], Nathan R. Thorp[1], Kirsten S. Hofmockel[5,6]

[1]Earth Systems Research Center, University of New Hampshire, Durham, New Hampshire, 03824, USA
[2]Soil and Water Management & Crop Nutrition Laboratory, FAO/IAEA Agriculture & Biotechnology Laboratories, Seibersdorf, Austria
[3]Department of Ecology, Evolution and Organismal Biology, Iowa State University, Ames, Iowa 50011, USA
[4] Northwest National Laboratory, Richland, Washington, 99354 USA
[5]Climate Change Science Institute and Environmental Sciences Division, Oak Ridge National Laboratory, Oak Ridge, Tennessee, 37831, USA
[6]Center for Accelerator Mass Spectrometry, Lawrence Livermore National Laboratory, Livermore, California, 94551, USA

Correspondence to: Erik A. Hobbie (erik.hobbie@unh.edu)

Abstract. We used $\delta^{15}N$ and $\delta^{13}C$ patterns from 16 peat depth profiles to interpret changes in C and N cycling in the Marcell S1 forested bog in northern Minnesota over the past ~10,000 years. In multiple regression analyses, $\delta^{15}N$ and $\delta^{13}C$ correlated strongly with depth, plot location, C/N, %N, and each other. Continuous variables in the regression model mainly reflected ^{13}C and ^{15}N fractionation accompanying N and C losses, with an estimated 40% of fractionations involving C-N bonds. In contrast, nominal variables such as plot, depth, and vegetation cover reflected peatland successional history and climate. Higher $\delta^{15}N$ and lower $\delta^{13}C$ in plots closer to uplands may reflect distinct hydrology and accompanying shifts in C and N dynamics in the lagg drainage area surrounding the bog. The Suess effect (declining $\delta^{13}CO_2$ since the Industrial Revolution) and aerobic decomposition lowered $\delta^{13}C$ in recent surficial samples. A decrease of 1‰ in the depth coefficient for $\delta^{15}N$ from -35 cm to -25 cm probably indicated the depth of ectomycorrhizal activity after tree colonization of the peatland. Low $\delta^{13}C$ at -213 cm and -225 cm (~8500 years BP) corresponded to a warm period during a sedge-dominated rich fen stage, whereas higher $\delta^{13}C$ thereafter reflected subsequent cooling. Because of multiple potential mechanisms influencing $\delta^{13}C$, there was no clear evidence for the influence of methanogenesis or methane oxidation on bulk $\delta^{13}C$.

1 Introduction

Carbon (C) and nitrogen (N) cycling are tightly linked (Schlesinger et al., 2011) and understanding the controls of C and N turnover in boreal peatlands is imperative to predict whether this ecosystem will continue to function as a strong C sink or change to a source of C, in the forms of atmospheric carbon dioxide (CO_2) and methane (CH_4), in the future. While 80-90% of C deposited in peatlands is lost via decomposition and microbial respiration in the upper aerobic layers of the acrotelm (Clymo, 1984), the deeper anaerobic catotelm accumulates recalcitrant *Sphagnum* litter and other organic matter due to low mineral nutrient availability and water-logged conditions. Carbon loss from the catotelm can be 50% within the first 1700 years with only an additional 15% over the next 5800 years (Kuhry and Vitt, 1996), thus making peatlands an important long-term C sink. Analysis of C and N in peatland cores is a potential way to determine key biochemical processes involved in organic matter burial and release.

Cores taken through the peat profile in peatlands trace the trajectory of peatland succession and contain the biogeochemical fingerprint of shifts in climate and peatland vegetation states. For example, groundwater-fed fen

Biogeosciences Discuss., doi:10.5194/bg-2016-261, 2016
Manuscript under review for journal Biogeosciences
Published: 6 September 2016
© Author(s) 2016. CC-BY 3.0 License.

peatlands and rainwater-fed bog peatlands differ in their pH, redox state, and balance of vascular plant versus *Sphagnum* abundance, with the transition from fens to bogs affecting biogeochemical processes and composition of organic matter throughout the peat profile (Vitt and Weider, 2006). Warming, drying, and increased N availability can also alter plant community composition, with concomitant effects on C and N dynamics, including enhanced production of greenhouse gases such as CO_2, CH_4, and nitrous oxide (N_2O) (Yavitt et al., 1987; Regina et al., 1996; Bergman et al., 1999; Juutinen et al., 2010).

Factors influencing C and N dynamics can be investigated using stable isotope measurements because biochemical and physical reactions proceed faster with lighter isotopes (^{12}C and ^{14}N) than with heavier isotopes (^{13}C and ^{15}N). As a result, different pools and fluxes can vary in their isotopic signatures (expressed as $\delta^{13}C$ and $\delta^{15}N$). Climate and foliar %N can also influence the $\delta^{13}C$ of photosynthesis by determining the relative rates of stomatal flux versus fixation of CO_2 (Brooks et al., 1998; Ménot and Burns, 2001; Sparks and Ehleringer, 1997). Radiocarbon measurements (^{14}C) are also important in biogeochemical research, as they allow dating of peat profiles and linking stable isotope patterns to specific climatic periods or vegetational phases of peatland succession. In peatlands, the dominant factors influencing organic C and N turnover can be identified by characterizing isotopic signatures of specific compounds or plant components through the peat profile (Nichols et al., 2009; Gavazov et al., 2016), but interpreting bulk peat signatures remains challenging. Deeper peats reflect both historic vegetation as well as accumulated effects of anaerobic fermentation occurring over thousands of years. In contrast, aerobic decomposition in shallower peats alters biogeochemistry over shorter time scales.

Our conceptual model of C and N dynamics during peatland succession is shown in Figure 1. Methanogenesis, methanotrophy, refixation of methane-derived CO_2, and plant composition influence the $\delta^{13}C$ of surficial layers (Ficken et al., 1998; Pancost et al., 2000), and the resulting $\delta^{13}C$ signal is over time transferred to deeper layers. Topography will also influence $\delta^{13}C$ because oxygen availability decreases with increasing water depth, resulting in different levels of methanogenesis and methanotrophy in hummocks versus hollows. Topography further influences $\delta^{13}C$ because for equivalent depths below the mean bog surface hummock C is older than hollow C.

Differential rates of NPP and decomposition which vary by specific vegetation and water table could also contribute to topographic effects (Moore et al., 2007; Wieder et al., 2009). The anthropogenic addition of ^{13}C-depleted CO_2 to the atmosphere via the burning of fossil fuels (the Suess effect, Ehleringer et al., 2000) also increases the gradient between ^{13}C-depleted surficial horizons and older, ^{13}C-enriched deeper horizons.

How N dynamics will influence $\delta^{15}N$ patterns is also shown in Figure 1. In aerobic soils, uptake by mycorrhizal fungi and subsequent transfer of ^{15}N-depleted N to host plants increases the ^{15}N divergence between deeper, ^{15}N-enriched horizons and surficial horizons (Hobbie and Ouimette, 2009), with such processes presumably not operating in *Sphagnum* and deep-rooted nonmycorrhizal plants (Kohzu et al., 2003). Nitrogen transport from uplands can be considerable in the lagg drainage region surrounding a peatland (Verry and Janssens 2011), and depending on the drainage $\delta^{15}N$, may influence the $\delta^{15}N$ of the receiving peatland. For example, lagg drainage could contribute ^{15}N-depleted nitrate or dissolved organic N (DON) (Yano et al., 2009), that differ isotopically from N fixation (0‰) or atmospheric N inputs (Stewart et al., 1995; Högberg 1997). In addition, biogeochemical hotspots are important for N dynamics in peatlands (Hill et al., 2016). Microbial processing of organic matter in soils commonly increases the $\delta^{15}N$ and $\delta^{13}C$ of the residual material (Nadelhoffer and Fry, 1994), although a N loss mechanism must also be present for $\delta^{15}N$ to be affected. Such processing decreases the C/N of organic matter, since respiratory C losses are generally greater than N losses.

Here, we used $\delta^{15}N$, $\delta^{13}C$, %N, and %C patterns of peat profiles, plant tissues, and fungal hyphae sampled from the Spruce and Peatland Responses Under Climatic and Environmental Change (SPRUCE) experimental site in northern Minnesota at the Marcell S1 bog (prior to initiation of a global change experiment, Iversen et al., 2014) to investigate potential factors influencing C and N turnover in peatlands. In addition to the continuous variables of elemental concentration and isotopic signatures, nominal variables included plot location, depth, topography (hummock versus hollow), and vegetation (near trees or not). We used concurrent radiocarbon measurements (McFarlane et al., *submitted*) to link the stable isotope measurements to the 11,000-year history of C and N dynamics at the SPRUCE experimental site. With this combination of data, we studied how *in situ* biogeochemistry and peatland succession may have influenced the isotopic profiles. We inferred the path of peatland succession from a prior study of the nearby S2 bog, as given in Table 1.

Biogeosciences Discuss., doi:10.5194/bg-2016-261, 2016
Manuscript under review for journal Biogeosciences
Published: 6 September 2016
© Author(s) 2016. CC-BY 3.0 License.

Isotopic patterns reflect the sum total of numerous factors. Specifically, we address five potential drivers of isotopic variation:

(1) in upper peat layers, ^{13}C depletion will reflect anthropogenic declines in the $\delta^{13}C$ of atmospheric CO_2 (Suess effect);

(2) microbial processing and biochemical composition (as inferred from %N, %C, and C/N) will influence peatland $\delta^{13}C$ and $\delta^{15}N$;

(3) proximity to uplands will increase N concentrations and peat $\delta^{15}N$;

(4) climatic patterns during the Holocene may influence peatland $\delta^{13}C$;

(5) methanogenesis in peat profiles during periods of high sedge abundance will enrich ^{13}C in peat whereas during periods of low sedge abundance methanotrophy combined with subsequent CO_2 assimilation by *Sphagnum* will deplete ^{13}C in peat.

2 Methods

2.1 Site description

Soil and fungal samples were collected from the SPRUCE experimental site at the S1 bog in the USDA Forest Service Marcell Experimental Forest in northern Minnesota, USA (47° 30.476'N, 93° 27.162'W). The bog is dominated by the trees *Picea mariana* (Mill.) Britton, Sterns and Poggenb. and *Larix laricina* (Du Roi) K.Koch, ericaceous shrubs (*Ledum groenlandicum* Oeder; *Chamaedaphne calyculata* (L.) Moench.) and *Sphagnum* mosses. Various forbs and sedges are also present. The bog micro-topography can be separated into hummocks (protruding above the average water table) and depressed hollows, and divided into areas with trees (*Picea* or *Larix*) or without trees. Average annual air temperature from 1961 to 2005 was 3.3°C with yearly mean extremes of -38°C and 30°C and average annual precipitation of 768 mm (Sebestyen et al., 2011). Average pH of the peat is 4.1 and average gravimetric water content is 7.40 g H_2O g^{-1} dry peat (Iversen et al., 2014).

2.2 Procedures

Peat cores for this analysis were collected in mid-August of 2012 from locations along three boardwalks extending out into the bog beyond the lagg region (Figure 2). Surface peat (~0–30 cm) was collected using a modified hole saw, while deeper peat down to mineral soil (~30–250 cm) was collected using a Russian peat corer. Cores were taken in both hummocks and hollows, with 0 cm defined as the surface of hollows and hummock heights above that assigned positive depths. Cores were bulked and homogenized every 10 cm over the 0 to -100 cm depth, every 25 cm from -100 to -200 cm, and over the entire 50 cm increment from -200 to -250 cm (in some cases, -300 cm was reached before mineral soil was observed). Cores were sampled at 17 locations (Figure 2; the locations of future experimental plots distributed across the three boardwalks) and material from 16 of these locations was used for the $\delta^{13}C$, $\delta^{15}N$, and radiocarbon measurements reported here. At locations 4, 5, 6, and 7 along the southern boardwalk, separate cores were taken within 150 cm of *Picea* or *Larix* trees and in the open (no trees within 150 cm), and the distinction designated as 'treed' or 'untreed'.

Peat cores were analyzed for $\Delta^{14}C$, $\delta^{13}C$, $\delta^{15}N$, %C, %N, and C/N by depth increment, with the depth increment recorded as the average depth (for example, 0 to 10 cm in a hummock given as 5 cm). Peat cores were analyzed in hummocks to a depth of -10 cm and in hollows to the bottom of the core (between -200 and -300 cm). Live woody plant foliage and fine roots to -10 cm were collected in August 2012 and live *Sphagnum* in 2013.

To collect fungal hyphae, in-growth cores were constructed. Mesh (40 µm) in-growth bags (10 cm × 10 cm) were filled with sterile sand. Bags were incubated in the field in paired hummock and hollows at six locations in the bog. In hummocks, bags were inserted at +10 to 0 cm above the adjacent hollow and in both locations from 0 to -10 cm and -10 to -20 cm below the hollow surface. Bags were installed on June 5, 2013 and recovered on September 20, 2013. Sand from in-growth bags was combined with ultrapure water and mixed at 80 rpm for 20 minutes. Suspended hyphae were removed with tweezers and the process was repeated until all hyphae were collected. Hyphal biomass was dried in the oven at 60ºC for 48 hours. Of 30 in-growth samples, 20 generated enough hyphal mass for analysis. All 20 samples were treated as independent replicates in statistical analyses.

Biogeosciences Discuss., doi:10.5194/bg-2016-261, 2016
Manuscript under review for journal Biogeosciences
Published: 6 September 2016
© Author(s) 2016. CC-BY 3.0 License.

2.3 Isotopic and elemental analysis

Radiocarbon content of homogenized bulk peat was measured on the Van de Graaff FN accelerator mass spectrometer (AMS) at the Center for AMS at Lawrence Livermore National Laboratory. Peat samples were not chemically pretreated prior to ^{14}C measurement. Samples were prepared by sealed-tube combustion to CO_2 in the presence of CuO and Ag and then reduced onto Fe powder in the presence of H_2 (Vogel et al.,, 1984). Radiocarbon isotopic values had an average AMS precision of 2.6‰ and were corrected for mass-dependent fractionation with $\delta^{13}C$ values from analyses conducted at the Department of Geological Sciences Stable Isotope Laboratory at University of California-Davis using a GVI Optima Stable Isotope Ratio Mass Spectrometer. Radiocarbon values are reported here in $\Delta^{14}C$ notation corrected for ^{14}C decay since 1950 (Stuiver and Polach, 1977). Calibrated ages were determined using Calib (http://calib.qub.ac.uk/calib/) or CaliBomb (Reimer et al., 2004) with INTCAL13 (Reimer et al., 2013) and Northern Hemisphere Zone 1 bomb curve extension (Hua et al., 2013) atmospheric ^{14}C calibration curves. Years before present (BP) refer to years prior to 1950. For more recent samples, calendar years AD may also be used.

These same soil samples and additional samples of hyphae and foliage were analyzed for %C, %N, $\delta^{13}C$, and $\delta^{15}N$ at the University of New Hampshire Stable Isotope Laboratory using a Costech 4010 Elemental Analyzer coupled to a Thermo Delta Plus XP IRMS. Standard deviations of laboratory standards (tuna, NIST 1515, and NIST 1575a) for $\delta^{15}N$ and $\delta^{13}C$ averaged less than 0.2‰. Fine roots of the woody vascular plants were analyzed for their stable isotopic composition at the Oak Ridge National Laboratory on an Integra CN mass spectrometer (SerCon, Crewe, UK), using standards traceable to NIST 8547-ammonium sulfate or 8542-sucrose (NIST, Gaithersburg, Maryland, USA).

2.4 Statistical tests

The statistical program JMP (SAS Institute, Middleton, Massachusetts, USA) was used for statistical analyses. Reported values are ± standard error, unless otherwise specified. Regression models for soil $\delta^{13}C$ and $\delta^{15}N$ were tested. Factors included in the regression model included nominal variables of vegetation type (treed or non-treed) and topography (hollow or hummock). Plot number and depth were also treated as nominal variables. As a nominal variable, depths with only a single measurement were generally excluded, unless they were very similar in depth to another value. Continuous variables included %N, %C, and isotopic values.

To test whether plot location, proximity to trees, depth, topography, and elemental concentrations influenced the carbon and N isotope patterns in peat profiles, we used multiple regression analyses. Sample %C, %N, and either $\delta^{13}C$ or $\delta^{15}N$ were included as continuous variables. Because the effects of depth or plot location on N and C dynamics are unlikely to change continuously (for example, methanogenesis requires an anaerobic soil and plots at bog edges may have different hydrology and N dynamics than plots in the middle of the bog, Urban and Eisenreich, 1988), depth and plot were treated as nominal (categorical) variables in our regression models. Within a given depth, values for radiocarbon were tested for correlations against $\delta^{13}C$ and $\delta^{15}N$ and the slope of the regression estimated.

3 Results

3.1 $\delta^{13}C$ and $\delta^{15}N$ in plants and fungal hyphae

Of the six vascular plant taxa tested, $\delta^{13}C$ of foliage varied from -30‰ in *Larix* to -28‰ in *Picea*. The $\delta^{15}N$ of plant foliage varied more widely than $\delta^{13}C$, from -8.5‰ for *Picea* to 2.5‰ for *Eriophorum*. Fine root $\delta^{13}C$ averaged -27.4±0.3‰ for *Larix*, -26.9±0.1‰ for *Picea*, and -28.5±0.2‰ for shrubs. Fine root $\delta^{15}N$ averaged -4.7±0.4‰ for *Larix*, -4.1±0.3‰ for *Picea*, and -1.8±0.1‰ for shrubs, whereas coarse roots of shrubs averaged -3.4±0.3‰. If we assume plant productivity patterns are similar aboveground and belowground, then the productivity-weighted average in vascular plants for $\delta^{13}C$ was -29.2‰ for foliage and -27.3‰ for roots (Table 2). Fungal hyphae from in-growth cores (n = 20) averaged -26.0±0.2‰ (se) for $\delta^{13}C$ and -0.3±0.2‰ for $\delta^{15}N$.

Biogeosciences Discuss., doi:10.5194/bg-2016-261, 2016
Manuscript under review for journal Biogeosciences
Published: 6 September 2016
© Author(s) 2016. CC-BY 3.0 License.

3.2 $\delta^{13}C$ and $\delta^{15}N$ in peat profiles

Carbon isotope ($\delta^{13}C$) values of peat in the profile increased from -29‰ in the top 10 cm of hummocks and hollows to -26‰ at -112 cm and then decreased slightly at greater depths. $\delta^{13}C$ values changed most rapidly from 0 cm to -50 cm depth (Figure 3a). Nitrogen isotope values in the peat profile increased from -3‰ in hummocks above the water level to around 1‰ at -50 cm. $\delta^{15}N$ then decreased to 0‰ at -85 cm before increasing again to 1.5‰ at -200 cm. Similar to $\delta^{13}C$, $\delta^{15}N$ changed most rapidly from 0 cm to -50 cm depth (Figure 3b).

In a regression model for $\delta^{13}C$ including $\delta^{15}N$, C/N, %N, and %C as continuous variables and the vegetation type, topography, plot sampling location, and depth as nominal variables, all factors were statistically significant. The model explained 86% of the total variance (n = 238, adjusted r^2) in peat $\delta^{13}C$. Depth explained 49%, %N explained 12%, C/N and $\delta^{15}N$ each explained 11%, plot explained 10%, and the remaining three variables together explained just 7% of the variance (Table 3). In the regression model, plot 17 was significantly higher and plots 4, 5, and 19 were significantly lower than the mean for $\delta^{13}C$. The complete regression models for $\delta^{13}C$ and $\delta^{15}N$ are given in Appendix 1.

A regression model for $\delta^{15}N$ of peat included $\delta^{13}C$, C/N, %N, and %C as continuous variables and the vegetation type, topography, plot, and depth as nominal variables. This model explained 70% of the total variance (adjusted r^2). Of the explained variance, depth accounted for 39%, %N 15%, $\delta^{13}C$ and plot 14% each, C/N 10%, and the remaining three variables accounted for 9% (Table 3). For $\delta^{15}N$, plots 4, 9, and 19 were significantly above 0‰ and plot 11 was significantly below 0‰. Hollows were lower than hummocks by 0.64‰ in $\delta^{13}C$ ($p = 0.007$) and by 1.42‰ in $\delta^{15}N$ ($p = 0.008$), and cores near trees were lower by 0.30‰ in $\delta^{13}C$ ($p = 0.014$) and higher by 0.58‰ in $\delta^{15}N$ ($p = 0.029$) than those without trees.

The coefficients for the nominal variable of depth and plot in models explaining $\delta^{13}C$ and $\delta^{15}N$ values are plotted in Figure 4 and Figure 5, respectively. Coefficients for depth were negative above the water table, increased regularly from -5 cm to -25 cm, and then varied little in $\delta^{13}C$ in the deepest horizons while still increasing in $\delta^{15}N$. For $\delta^{13}C$, most depth coefficients differed significantly from 0 except at 5, -15, and below -162 cm, whereas for $\delta^{15}N$, all depth coefficients differed significantly from 0 except at -25 cm, -65, -85 cm, and below -225 cm. The depth coefficients for $\delta^{13}C$ and $\delta^{15}N$ were positively correlated (adjusted $r^2 = 0.306$, $n = 17$, $P = 0.0125$, $\delta^{15}N = 1.64\pm0.58 \times \delta^{13}C + 0.00\pm0.43$) (Figure 4). The coefficients for the nominal variable of plot in models explaining $\delta^{13}C$ and $\delta^{15}N$ values were negatively correlated (adjusted $r^2 = 0.279$, $p = 0.02$, $\delta^{15}N = -1.34\pm0.51 \times \delta^{13}C + 0.07\pm0.08$, Figure 5a). There was some spatial patterning of values, with plots near to the western upland high in $\delta^{15}N$ and low in $\delta^{13}C$, and other plots showing the opposite pattern (Figure 5b).

Although overall patterns of radiocarbon with depth were clear, radiocarbon varied widely at any given depth, and correlated significantly with $\delta^{13}C$ or $\delta^{15}N$ at several depths (Table 4). Radiocarbon correlated positively with $\delta^{13}C$ at -163 cm, -5 cm, 5 cm, and 15 cm, and correlated negatively with $\delta^{13}C$ at -35 cm and -65 cm. In contrast, radiocarbon correlated positively with $\delta^{15}N$ at -65 cm, -55 cm, -45 cm, - 5 cm, and 15 cm, and correlated negatively with $\delta^{15}N$ at -162 cm and -25 cm. Overall patterns of $\Delta^{14}C$ with $\delta^{13}C$ or $\delta^{15}N$ are shown in Figure 6a and Figure 6b, respectively.

4 Discussion

4.1 Potential causes of shifts in $\delta^{13}C$ and $\delta^{15}N$ in peat profiles

Isotopic ratios within the profile can shift if elemental fluxes in or out of the system differ isotopically from profile material (Figure 1). Loss of labile C via respiration, methanogenesis, or leaching (Kolka et al., 1999) could alter the $\delta^{13}C$ of the residual material, as could inputs of ^{13}C-enriched material such as roots or mycorrhizal hyphae. Similarly, changes in the $\delta^{13}C$ of atmospheric CO_2 can alter the $\delta^{13}C$ of photosynthetically fixed C whereas changes in moisture, temperature, or photosynthetic capacity can alter the ^{13}C discrimination between atmospheric CO_2 and fixed C. For N, loss of ^{15}N-depleted material from the bulk peat via mycorrhizal transfer to fine roots, direct root uptake, denitrification, or leaching of organic or inorganic N could raise the $\delta^{15}N$ of the remaining soil organic matter. Inputs of N via atmospheric deposition, N fixation, or transport from surrounding uplands could also

Biogeosciences Discuss., doi:10.5194/bg-2016-261, 2016
Manuscript under review for journal Biogeosciences
Published: 6 September 2016
© Author(s) 2016. CC-BY 3.0 License.

influence $\delta^{15}N$ if these inputs differ isotopically from peat profile values. These processes can be linked to past climate and vegetation with profile radiocarbon measurements that are calibrated to calendar years. Here, we used radiocarbon to indicate the potential timing of shifts in some of the primary drivers that influenced C and N stable isotope patterns within the peat profiles at SPRUCE. We will first discuss quantitative factors within the framework of our multiple regressions of $\delta^{13}C$ and $\delta^{15}N$, then discuss the categorical variables of vegetation cover, topography, plot, and depth.

4.2 %N, %C, and C:N stoichiometry influence $\delta^{13}C$ and $\delta^{15}N$ patterns

%N, %C, and C/N contributed 26% and 29% of explained variance, respectively, to our regression models of $\delta^{15}N$ and $\delta^{13}C$. These factors reflect the biochemical and isotopic composition of the original plant material, or may reflect how the chemical structure and isotopic composition of plant material has altered during its slow decomposition at S1.

Microbially-driven C loss raises soil organic matter %N, lowers C/N, and enriches soil organic matter in ^{13}C (resulting from loss of ^{13}C-depleted CO_2) (Ehleringer et al., 2000; Alewell et al., 2011). The positive correlation of %N with $\delta^{13}C$ may therefore reflect an underlying correlation between the accumulation of ^{13}C-enriched microbial necromass (Wallander et al., 2004) and the increased N content of the peatland organic matter. Fungal %N and $\delta^{13}C$ are positively correlated (Hobbie et al., 2012) because of the high $\delta^{13}C$ of microbially synthesized protein relative to other microbial components such as carbohydrates and lipids. In contrast, the positive correlation of C/N with $\delta^{13}C$ and negative correlation with $\delta^{15}N$ presumably reflects a legacy of buried wood, which, relative to other plant material, should be high in $\delta^{13}C$ (Trudell et al., 2004) and high in C/N. This can be seen clearly in the few samples with C/N greater than 70, which is higher than any plant tissue measured in this study. Although some *Sphagnum* taxa under pristine conditions can be very low in %N and $\delta^{15}N$ and high in C/N (Asada et al., 2005a), here, the presence of wood was noted seven times during laboratory examination of samples, with those samples twice as high in C/N (average, 69) as other samples, and were also significantly higher in C/N in multiple regression analysis (see Appendix 2).

The negative correlation of %N with $\delta^{15}N$ indicated that either added or removed N is low in $\delta^{15}N$. One possibility for removal is that ^{15}N-depleted N has been transferred from mycorrhizal fungi to plants and subsequently lost during fire or as DON after decomposition at the surface. By removing the surficial, ^{15}N-depleted litter horizons, fire enriches the soil profile in ^{15}N (Hobbie and Högberg, 2012). Alternatively, N could be added via fixation with a $\delta^{15}N$ value of -1‰, which would lower overall $\delta^{15}N$ values deeper in the peat profile. However, we point out that only at -45 cm and -55 cm are %N and $\delta^{15}N$ significantly and negatively correlated (Appendix 3). At these depths, %N is about 1.8% and $\delta^{15}N$ is about 1‰ (Figures 3b, d). The value of the coefficient for %N in the $\delta^{15}N$ regression, -2.6‰/%N, implied that the perturbing N has a $\delta^{15}N$ value that is 1.8% × 2.6‰/% less than that of 1‰, or -3.68‰, which is too low to be fixed N. The apparent ^{15}N depletion of 4.7‰ against the source N is a plausible value for ^{15}N discrimination between mycorrhizal fungi and host plants (Hobbie and Colpaert, 2003). In addition, DON appears to be higher in $\delta^{15}N$ than bulk peat (Broder et al., 2012), so DON losses could not cause a ^{15}N enrichment of the remaining N. It also implies that N fixation must be above this depth, which agrees with the apparent coupling of N fixation and *Sphagnum* activity (Bragina et al., 2012; Sanna et al., 2015).

The negative correlation of %C with $\delta^{13}C$ is expected based on the chemical composition of ^{13}C-depleted compound classes of lignin, aromatics, and lipids, which are high in %C (Poorter et al., 1997; Hobbie et al., 2002). Initial decomposition of *Sphagnum* commonly decreases $\delta^{13}C$, as ^{13}C-enriched soluble components are leached (Asada et al., 2005b). In contrast, aromatics and lipids do not generally contain N, so the positive correlation of %C with $\delta^{15}N$ in bulk peat cannot be explained in the same manner. However, microbial processing generally enriches soils in ^{15}N (Billings and Richter 2006; Templer et al., 2007) while increasing %C, which was also true at S1 (Tfaily et al., 2014).

4.3 $\delta^{13}C$ and $\delta^{15}N$ patterns are linked

Biogeosciences Discuss., doi:10.5194/bg-2016-261, 2016
Manuscript under review for journal Biogeosciences
Published: 6 September 2016
© Author(s) 2016. CC-BY 3.0 License.

Information about the structure of the compounds isotopically fractionated during peat decomposition can be inferred from the relative effects of $\delta^{15}N$ and $\delta^{13}C$ in our regression models on $\delta^{13}C$ and $\delta^{15}N$. The positive effect of $\delta^{15}N$ on $\delta^{13}C$ values (slope, 0.177) and $\delta^{13}C$ on $\delta^{15}N$ values (slope, 0.882) is not surprising, since C:N bonds are ubiquitous in organic material and breaking a C:N bond will discriminate against both ^{13}C and ^{15}N. The coefficient of $\delta^{15}N$ in the multiple regression for $\delta^{13}C$ can be defined as $\delta^{15}N_{coeff}$ and can be expressed as:

$$\delta^{15}N_{coeff} = \varepsilon^{13C}/\varepsilon^{15N} \times f_{C:N} \quad \text{Eq. (1)}$$

where ε^{13C} and ε^{15N} are the ^{13}C and ^{15}N enrichments during C:N bond formation or breaking, and $f_{C:N}$ is the proportion of total C bonds fractionated that involve a C:N bond.

Similarly, we can write the coefficient for the effect of $\delta^{13}C$ on $\delta^{15}N$ as:

$$\delta^{13}C_{coeff} = \varepsilon^{15N}/\varepsilon^{13C} \times f_{N:C} \quad \text{Eq. (2)}$$

where $f_{N:C}$ is the proportion of total N bonds fractionated that involve a C:N bond. Combining these two equations results in:

$$\delta^{15}N_{coeff} \times \delta^{13}C_{coeff} = f_{C:N} \times f_{N:C} \quad \text{Eq. (3)}$$

Replacing $\delta^{15}N_{coeff}$ with 0.177 and $\delta^{13}C_{coeff}$ with 0.882 gives a value of $f_{C:N} \times f_{N:C}$ of 0.156, so on average 40% of bond fractionations ($0.156^{0.5}$) involve C:N bonds. Interestingly, comparable data were generated from $\delta^{15}N$ and $\delta^{13}C$ patterns in caps and stipes of mushrooms (Hobbie et al., 2012). In those multiple regressions, $\delta^{15}N_{coeff}$ was 0.121 and $\delta^{13}C_{coeff}$ was 0.853, so $f_{C:N} \times f_{N:C}$ would be 0.103 and on average 32% of bond fractionations ($0.103^{0.5}$) involved C:N bonds. The somewhat higher proportion of bond fractionations involving C:N bonds at S1 (40%) than in pure fungi (32%) may simply reflect the greater contributions to isotopic patterns of microbial biomass from Archaea and Bacteria at S1, since these latter taxa have higher N:C ratios and protein content than fungi, and therefore more peptide bonds. Since peptide bonds link C and N, peptide bond disruption will affect C and N bonds equally.

4.4 The Suess effect increases ^{13}C depletion in surficial peat

The strong dependence of $\delta^{13}C$ on peat depth partially reflects the 1.7‰ decline in the $\delta^{13}C$ of atmospheric CO_2 since 1850, with the lowest $\delta^{13}C$ values above the water table, where C is of recent origin. For example, the lowest values of depth coefficients (~-1‰) in hummocks at 15 cm, 22 cm, and 25 cm above the mean bog surface reflect C from the last 50 years, as confirmed by $\Delta^{14}C$ averages of 59‰, 29‰, and 52‰ for these three depths, where only C influenced by ^{14}C created during thermonuclear testing should have positive $\Delta^{14}C$ values (Table 4). Although our sampling lacked sufficient vertical resolution to explicitly include corrections for the Suess effect (e.g., as done in Esmeijer-Liu et al., 2012), the ~1.5‰ increase in the depth coefficient of our $\delta^{13}C$ regression model from the hummocks to deeper in the profile correspond well to the long-term shift in $\delta^{13}C$ of atmospheric CO_2 from pre-industrial times to the present. An additional factor contributing to the higher depth coefficient could be the 1-2‰ higher $\delta^{13}C$ in roots than in foliage and the different input depths of foliage (surface only) and roots (distributed throughout the acrotelm). The steady increase in the $\delta^{13}C$ coefficient between -5 cm and -25 cm depth presumably reflects the increasing dominance of pre-industrial C. Depths of -35 cm and below all had $\Delta^{14}C$ values less than -100‰ (Table 4), indicating primarily pre-bomb and pre-industrial C when the average $\delta^{13}C$ of atmospheric CO_2 was -6.5‰ (versus the current value of -8.2‰). In addition, modern production of organic matter averaged -29‰ in $\delta^{13}C$ (Table 2), similar to values for surficial horizons, whereas deeper horizons were between -27‰ and -26‰. The Suess effect of ~1.5‰ therefore accounted for at least half of this difference.

4.5 Proximity to uplands and trees increases peat $\delta^{15}N$

Biogeosciences Discuss., doi:10.5194/bg-2016-261, 2016
Manuscript under review for journal Biogeosciences
Published: 6 September 2016
© Author(s) 2016. CC-BY 3.0 License.

Plot-specific coefficients for $\delta^{13}C$ and $\delta^{15}N$ are negatively correlated (Figure 5a), and may therefore reflect site-specific differences in the dominance of conditions favoring ^{13}C- or ^{15}N-depleted losses during peatland development. The positive coefficients for $\delta^{15}N$ and negative coefficients for $\delta^{13}C$ are from the plots closest to the lagg region adjacent to the western upland. This suggests that the different hydrology in the lagg has enhanced ^{15}N fractionation from N removal mechanisms such as denitrification, nitrification, or leaching of DON. Alternatively, dissolved N transported from the uplands during spring thaw and melt may have provided an additional ^{15}N-enriched N source for these plots located near the bog edges (Figure 5b). Peatland DON appears enriched in ^{15}N and ^{13}C relative to bulk peat (Broder et al., 2012), and this is presumably true for upland sources as well. In the adjacent Marcell S2 kettle bog, large N fluxes from upland locations from both surface runoff and interflow led to much larger N losses in streamflow from the lagg region (~32 kg ha^{-1} yr^{-1}) than from the bog itself (2 kg ha^{-1} yr^{-1}) (Urban and Eisenreich, 1988). The uplands here are dominated by ectomycorrhizal trees such as *Populus*, *Quercus*, and *Pinus*, which tend to produce vertically stratified soil profiles with high $\delta^{15}N$ values in lower organic and mineral horizons (Hobbie and Ouimette, 2009). We therefore expect DON produced in uplands to be high in $\delta^{15}N$, which will serve as a source of ^{15}N-enriched N to lagg regions of peatlands. The greater vertical stratification of $\delta^{15}N$ possible with trees than with mosses may therefore also cause here the higher $\delta^{15}N$ coefficient for treed versus non-treed locations (Table 3), since higher levels of ^{15}N-depleted N in the active surficial layers should promote losses of this N and the ultimate ^{15}N enrichment of remaining N. In contrast, the lower $\delta^{13}C$ coefficient for treed versus non-treed locations suggests decreased surface wetness near trees and consequent greater ^{13}C discrimination by *Sphagnum* during photosynthesis (Kühl et al., 2010). Relative to *Sphagnum*, the high transpiration rates of trees relative to *Sphagnum* may reduce surface moisture.

4.6 Isotopic patterns with depth reflect climate and vegetation

Peatland succession and climate have been established previously at the nearby S2 bog and are summarized in Table 1. As the same climatological factors affected the S2 and S1 (SPRUCE) bogs, plant stratigraphy and isotopic patterns were probably similar, although accumulation rates are lower at S1 than at S2 (personal communication, E. Verry). Vegetation cover plays a role in $\delta^{13}C$ patterns, as sedges may cause $\delta^{13}C$ in peatlands to increase by promoting loss of ^{13}C-depleted methane, thereby increasing $\delta^{13}C$ of residual C, whereas mosses and associated methanotrophic bacteria may foster the retention of ^{13}C-depleted C in peatlands dominated by *Sphagnum* mosses (Larmola et al., 2010).

The high $\delta^{15}N$ and relatively low $\delta^{13}C$ at -213 cm and -225 cm corresponded approximately to a warm period between 8000 and 9200 BP, during a sedge-dominated rich fen stage (Verry and Janssens, 2011), with mean annual temperatures of 4-5°C. Higher temperatures in peatlands are associated with lower $\delta^{13}C$ values (Skryzpek et al., 2005, 2008).

In the following paragraphs, we will link shifts in $\delta^{15}N$ and $\delta^{13}C$ through the profile to radiocarbon ages and the corresponding patterns in vegetation and climate at the S2 bog. Radiocarbon and $\delta^{13}C$ correlated positively at -162 cm, corresponding to a 1‰ rise in $\delta^{13}C$ which accompanied a drop in MAT to perhaps 2°C by 6000 BP. This cooling trend was also accompanied by a slight rise in precipitation, so the decreased ^{13}C discrimination could also be attributed to increased *Sphagnum* moisture (Rice and Giles, 1996), although it is difficult to distinguish between these two possible causes of ^{13}C differences (Ménot and Burns, 2001). *Sphagnum* discrimination is less with increased moisture because CO_2 diffusion is limited under wet conditions. The stratigraphy at the S2 bog indicates a vegetational shift from a rich fen to a transitional fen during this period. The negative correlation between radiocarbon and $\delta^{15}N$ at this depth suggests decreasing losses of ^{15}N-depleted N during this vegetational transition.

Based on plant stratigraphy at the neighboring S2 bog, the depth increment from -85 cm to -112 cm corresponds to a transitional fen stage 3300-4800 years ago. In our regression model for $\delta^{13}C$, these two depths are about 0.5‰ higher in $\delta^{13}C$ than at -162 cm. The peak in $\delta^{13}C$ may reflect a phase during which sedges transported methane directly to the atmosphere, thereby minimizing the refixation in *Spaghnum* cells of ^{13}C-depleted, methanotrophic-derived carbon dioxide. An accompanying trough in $\delta^{15}N$ at -400‰ $\Delta^{14}C$ (4220 calibrated years BP, Figure 5) suggests that processes increasing $\delta^{13}C$ such as high sedge abundance may decrease sequestration of ^{15}N-enriched organic matter. One possible explanation is that systems with nonmycorrhizal sedges create less ^{15}N-depleted N in the active surficial horizons because of sedge uptake of deeper, ^{15}N-enriched N, as suggested by high

Biogeosciences Discuss., doi:10.5194/bg-2016-261, 2016
Manuscript under review for journal Biogeosciences
Published: 6 September 2016
© Author(s) 2016. CC-BY 3.0 License.

Eriophorum $\delta^{15}N$ relative to *Sphagnum* and other vascular plants (Table 2) and the deep root distribution of sedges relative to woody plants (Iversen et al., 2015). As a consequence, N losses from sedge systems will tend to be ^{15}N-enriched relative to N losses from systems without sedges.

The positive correlations between $\delta^{15}N$ and $\Delta^{14}C$ at -45, -55, and -65 cm (Table 4 and Figure 6b) may be linked to a parallel decline in %N over these time periods, so that younger samples are lower in %N and higher in $\delta^{15}N$ than older samples. This presumably reflects losses of ^{15}N-depleted N from the younger samples.

The cause for the drop of 1.4‰ in the $\delta^{15}N$ coefficient from -35 cm depth (modern) to -25 cm (~1000 yr BP) and greater depths is unclear; possibly, since there is no parallel increase in the $\delta^{13}C$ coefficient, this reflects long-term cycling and loss of N during denitrification, as suggested by Puglisi et al. (2014). However, nitrate is very low at this site (Iversen et al., submitted) and is very low in organic horizons in bogs in other studies (Bayley et al., 2005). Nonetheless, nitrification and denitrification are higher in fens than in bogs and should change $\delta^{15}N$ patterns along the core profile as the core reflects peatland succession and climatological changes (Regina et al., 1996; Bayley et al., 2005; Wray and Bayley 2007). At the nearby S2 bog, poor fen transitioned to forested bog between 1610 AD and 1864 AD, with a charcoal layer at S2 indicating that peat was consumed by fire during this period, precluding a more specific date for this transition (Kolka, 2011; Verry and Janssens, 2011).

Here, negative values of the depth coefficient for $\delta^{15}N$ in the hummocks (heights from 5 to 25 cm above the water table) reflect the low $\delta^{15}N$ of recent litter inputs from ectomycorrhizal and ericoid mycorrhizal plants to these layers, as seen in Table 2, and the ~6‰ higher value for fungal hyphae. Transfer to plants of ^{15}N-depleted N by ectomycorrhizal and ericoid mycorrhizal fungi creates this contrast between low plant $\delta^{15}N$ and high fungal $\delta^{15}N$ (Hobbie and Hobbie 2008; Hobbie and Högberg, 2012). However, the low contribution of ectomycorrhizal and ericoid mycorrhizal fungi to total plant uptake here compared to forest sites dominated by ectomycorrhizal fungi accounted for the lower ^{15}N enrichment between surficial layers and deeper layers here (~3‰) than in forest soils, which averaged a 9.6‰ enrichment between surficial and deeper soils for ectomycorrhizal forests (reviewed in Hobbie and Ouimette, 2009). A relatively small influence of N uptake by ectomycorrhizal and ericoid mycorrhizal trees and shrubs on profile $\delta^{15}N$ patterns was observed at the nearby Marcell S2 bog, where mosses contributed 75% of total plant uptake, herbaceous plants 13%, and mycorrhizal trees and shrubs 13% (Urban and Eisenreich, 1988).

4.7 Methanogenesis and methane oxidation

Although methanogenesis can under certain conditions influence the $\delta^{13}C$ of bulk profiles, as has been reported from Asian rice paddies (Becker-Heidmann and Scharpenseel, 1986), peatlands may be too rich in C for methanogenesis to shift $\delta^{13}C$ values in bulk peat sufficiently to distinguish them clearly from other C loss mechanisms. Annual methane fluxes at S1 are only 2.5% of the fluxes of carbon dioxide (personal communication, P. J. Hanson), so the expected ^{13}C shifts caused by methanogenesis will not greatly affect bulk $\delta^{13}C$. We conclude that given the multiple processes that can influence peatland $\delta^{13}C$, our bulk profile data do not allow us to determine the relative influence of methanogenesis and methane oxidation on $\delta^{13}C$ patterns. Possibly concurrent measurements of bulk deuterium isotopes could settle the issue, since methanogenesis will discriminate greatly against deuterium whereas aerobic C losses will not.

5 Conclusions

Numerous factors can influence $\delta^{13}C$ and $\delta^{15}N$ patterns in peatland profiles. Although the multiple potential interactions among climate, vegetation, and soil processes make definitive conclusions difficult, we identified several factors that influenced these isotopic patterns, including the Seuss effect, C and N stoichiometry, microbial processing, and proximity to uplands and trees. The challenge now is to put these processes into models of peatland development that includes vegetational succession and climatic drivers, such as the Holocene Peatland Model (Frolking et al., 2010), and adapt these models to make isotopic predictions that can be compared against data. Such model-data comparisons should continue to improve our ability to interpret isotopic patterns, as well as reveal areas where our model formulations are currently inadequate.

6 Data availability

© Author(s) 2016. CC-BY 3.0 License.

The data presented in this study are available in the appendices and through the Iversen et al. (2014) publication.

7 Supplement link (will be included by Copernicus)

The supplement related to this article is available online at http://dx.doi.org/10.3334/CDIAC/spruce.025

Hofmockel, K.S., Chen, J. and Hobbie, E.A. 2016. SPRUCE S1 Bog Pretreatment Fungal Hyphae Carbon and Nitrogen Concentrations and Stable Isotope Composition from In-growth Cores, 2013-2014. Carbon Dioxide Information Analysis Center, Oak Ridge National Laboratory, Oak Ridge, Tennessee, USA. DOI: 10.3334/CDIAC/spruce.025

8 Author contributions

Samples were collected by C. Iversen, P. Hansen, and K. Hofmockel and analyzed by J. Chen, E. Hobbie, C. Iversen, and K. McFarlane. E. Hobbie prepared the manuscript with contributions from all authors.

9 Acknowledgements

The authors appreciate field sampling efforts of members of the SPRUCE research group, in particular Jana Phillips, Deanne Brice, and Joanne Childs. This material is based upon work supported by grant ER65430 to Iowa State University from the U.S. Department of Energy and the SPRUCE experiment is supported by the U.S. Department of Energy, Office of Science, Office of Biological and Environmental Research. This manuscript has been authored by UT-Battelle, LLC under Contract No. DE-AC05-00OR22725 with the U.S. Department of Energy. The United States Government retains and the publisher, by accepting the article for publication, acknowledges that the United States Government retains a non-exclusive, paid-up, irrevocable, world-wide license to publish or reproduce the published form of this manuscript, or allow others to do so, for United States Government purposes. The Department of Energy will provide public access to these results of federally sponsored research in accordance with the DOE Public Access Plan (http://energy.gov/downloads/doe-public-access-plan). The data referenced in this paper are archived at and available from the SPRUCE long-term repository (Iversen et al., 2014; http://mnspruce.ornl.gov).

Biogeosciences Discuss., doi:10.5194/bg-2016-261, 2016
Manuscript under review for journal Biogeosciences
Published: 6 September 2016
© Author(s) 2016. CC-BY 3.0 License.

10 References

Alewell, C., Giesler, R., Klaminder, J., Leifeld J., and Rollog, M.: Stable carbon isotopes as indicators for environmental change in palsa peats. Biogeosciences, 8, 1769-1778, doi:10.5194/bg-8-1769-2011, 2007.

Asada, T., Warner, B. G., and Aravena, R.: Nitrogen isotope signature variability in plant species from open peatland. Aquat. Bot., 297-307, 2005a.

Asada, T., Warner, B., and Aravena, R.: Effects of the early stage of decomposition on change in carbon and nitrogen isotopes in *Sphagnum* litter. J. Plant Interact., 1, 229-237, 2005b.

Bayley, S. E., Thormann, M. N., and Szumigalski, A. R.: Nitrogen mineralization and decomposition in western boreal bog and fen peat. Ecoscience, 12, 455-465, 2005.

Becker-Heidmann, P. and Scharpenseel, H. W.: Thin-layer $\delta^{13}C$ and $\Delta^{14}C$ monitoring of lessive soil profiles. Radiocarbon, 28, 383-390, 1986.

Bergman, I., Lundberg, P., and Nilsson, M.: Microbial carbon mineralisation in an acid surface peat: effects of environmental factors in laboratory incubations. Soil Biol. Biochem., 31, 1867-1877, 1997.

Billings, S. A. and Richter, D. D.: Changes in stable isotopic signatures of soil nitrogen and carbon during 40 years of forest development. Oecologia, 148, 325-33, doi:10.1007/s00442-006-0366-7, 2006.

Bragina, A., Maier, S., Berg, C., Müller, H., Chobot, V., Hadacek, F., and Berg, G. Similar diversity of Alphaproteobacteria and nitrogenase gene amplicons on two related Sphagnum mosses. Front. Microbiol., 2, 275. doi:10.3389/fmicb.2011.00275, 2012.

Bridgham S.D., Updegraff, K., Pastor J.: Carbon, nitrogen, and phosphorus mineralization in northern wetlands. Ecology, 79, 1545-1561, 1998.

Broder, T., Blodau, C., Biester, H., Knorr, K., and Conant, R.: Peat decomposition records in three pristine ombrotrophic bogs in southern Patagonia. Biogeosciences, 9, 2012.

Brooks, J. R., Flanagan, L. B., and Ehleringer, J. R.: Responses of boreal conifers to climate fluctuations: indications from tree-ring widths and carbon isotope analyses. Can. For. Res., 28, 524-533, 1998.

Ehleringer, J. R., Buchmann, N., and Flanagan, L. B.: Carbon isotope ratios in belowground carbon cycle processes. Ecol. Appl., 412-422, doi:10.2307/2641103, 2000.

Ficken, K. J., Barber, K. E., and Eglinton, G.: Lipid biomarker, $\delta^{13}C$ and plant macrofossil stratigraphy of a Scottish montane peat bog over the last two millennia. Org. Geochem., 28, 217-237, 1998.

Gavazov, K., Hagedorn, F., Buttler, A., Siegwolf R., and Bragazza L.: Environmental drivers of carbon and nitrogen isotopic signatures in peatland vascular plants along an altitude gradient. Oecologia, 180, 257-264, 2016.

Hill, B. H., Jicha, T. M., Lehto, L. L., Elonen C. M., Sebestyen S. D., and Kolka R. K..: Comparisons of soil nitrogen mass balances for an ombrotrophic bog and a minerotrophic fen in northern Minnesota. Sci. Total Environ., 550, 880-892, 2016.

Hobbie, E. A. and Colpaert, J. V.: Nitrogen availability and colonization by mycorrhizal fungi correlate with nitrogen isotope patterns in plants. New Phytol., 151, 115-126, 2003.

Hobbie, E. A. and Hobbie, J. E.: Natural abundance of ^{15}N in nitrogen-limited forests and tundra can estimate nitrogen cycling through mycorrhizal fungi: A review. Ecosystems, 11, 815-830. doi:10.1007/s10021-008-9159-7, 2008.

Hobbie, E. A. and Högberg, P.: Nitrogen isotopes link mycorrhizal fungi and plants to nitrogen dynamics New Phytol. 196, 367-382. doi:10.1111/j.1469-8137.2012.04300.x, 2012.

Hobbie, E.A. and Ouimette, A.P.: Controls of nitrogen isotope patterns in soil profiles. Biogeochemistry, 95, 355-371, 2009.

Hobbie, E. A., Tingey, D. T., Rygiewicz, P. T., Johnson, M. G., and Olszyk, D. M.: Contributions of current year photosynthate to fine roots estimated using a ^{13}C-depleted CO_2 source. Plant Soil 247, 233-242, 2002.

Hobbie, E. A., Sánchez, F. S., and Rygiewicz, P. T.: Controls of isotopic patterns in saprotrophic and ectomycorrhizal fungi. Soil Biology Biochemistry, 48, 60-68, 2012.

Högberg, P.: ^{15}N natural abundance in soil-plant systems. New Phytol., 137, 179-203, 1997.

Hua, Q., Barbetti, M., and Rakowski, A.: Atmospheric radiocarbon for the period 1950-2010. Radiocarbon, 55, 2059-2072, 2013.

Iversen, C. M., Hanson, P. J., Brice, D. J., Phillips, J. R., McFarlane, K. J., Hobbie, E. A., and Kolka, R. K., 2014. SPRUCE peat physical and chemical characteristics from experimental plot cores, 2012. Carbon Dioxide Information Analysis Center, Oak Ridge National Laboratory, U.S. Department of Energy, Oak Ridge, Tennessee, USA http://dx.doi.org/10.3334/CDIAC/spruce.005.

Iversen, C. M., Sloan, V. L., Sullivan, P. F., Euskirchen, E. S., McGuire, A. D., Norby, R. J., Walker, A. P., Warren,

© Author(s) 2016. CC-BY 3.0 License.

J. M., and Wullschleger, S. D.: The unseen iceberg: plant roots in arctic tundra. New Phytol., 205, 34-58, 2015.
Iversen, C. M., Childs, J., Norby, R. J., Ontl, T. A., Kolka, R. K., Brice, D. J., McFarlane, K. J., and Hanson, P. J.: Submitted. The distribution and dynamics of fine roots in a forested bog. Submitted to Ecology.
Kohzu, A., Matsui, K., Yamada, T., Sugimoto, A., and Fujita, N.: Significance of rooting depth in mire plants: Evidence from natural (^{15}) N abundance. Ecol. Res., 18, 257-266, 2003.
Kolka, R. K., Grigal, D. F., Verry, E. S., and Nater, E. A.: Mercury and organic carbon relationships in streams draining forested upland/peatland watersheds. J. Environ. Qual., 28, 766-775, 1999.
Krassovski, M. B., Riggs, J. S., Hook, L. A., Nettles, W. R., Boden, T. A., and Hanson, P. J.: A comprehensive data acquisition and management system for an ecosystem-scale peatland warming and elevated CO_2 experiment. Geosci. Instrum. Method. Data Syst., 4, 203–213, doi:10.5194/gi-4-203-2015, 2015.
Kühl, N., Moschen, R., Wagner, S., Brewer, S., and Peyron, O.: A multiproxy record of late Holocene natural and anthropogenic environmental change from the Sphagnum peat bog Dürres Maar, Germany: implications for quantitative climate reconstructions based on pollen. J. Quat. Sci., 25, 675-688, 2013.
Kuhry, P. and Vitt, D.H.: Fossil carbon/nitrogen ratios as a measure of peat decomposition. Ecology, 77, 271-275, 1996.
Larmola, T., Tuittila, E. S., Tiirola, M., Nykänen, H., Martikainen, P. J., Yrjälä, K., Tuomivirta, T., and Fritze, H.: The role of *Sphagnum* mosses in the methane cycling of a boreal mire. Ecology, 91, 2356-2365, 2010.
Leppänen, S. M., Rissanen , A. J., Tiirola, M.: Nitrogen fixation in *Sphagnum* mosses is affected by moss species and water table level. Plant Soil, 389, 185-196, 2015.
McFarlane, K. J., Iversen, C. M., Phillips, J. R., Brice, D. J., and Hanson, P.: Temporal and spatial heterogeneity of Holocene carbon accumulation in an ombrotrophic northern Minnesota bog. The Holocene submitted, 2016.
Ménot, G. and Burns, S. J.: Carbon isotopes in ombrogenic peat bog plants as climatic indicators: calibration from an altitudinal transect in Switzerland. Org. Geochem., 32, 233-245, 2001.
Moore, T. R., Bubier, J. L., and Bledzki, L.: Litter decomposition in temperate peatland ecosystems: the effect of substrate and site. Ecosystems, 10, 949-963, 2007.
Nichols, J. E., Walcott, M., Bradley, R., Pilcher, J., and Huang, Y.: Quantitative assessment of precipitation seasonality and summer surface wetness using ombrotrophic sediments from an Arctic Norwegian peatland. Quat. Res., 72, 443-45, 2009.
Pancost, R. D., van Geel, B., Baas, M., and Damste, J. S. S.: $\delta^{13}C$ values and radiocarbon dates of microbial biomarkers as tracers for carbon recycling in peat deposits. Geology, 28, 663-666, 2000.
Poorter, H., Berkel, Y., Baxter, R., Hertog. J. D., Dijkstra, P., Gifford, R., Griffin, K., Roumet, C., Roy, J., and Wong, S.: The effect of elevated CO_2 on the chemical composition and construction costs of leaves of 27 C_3 species. Plant Cell Environ., 20, 472-482, 1997.
Puglisi, E., Zaccone, C., Cappa, F., Cocconcelli, P. S., Shotyk, W., Trevisan, M., and Miano, T. M.: Changes in bacterial and archaeal community assemblages along an ombrotrophic peat bog profile. Biol. Fertil. Soils, 50, 815-826, 2014.

Regina, K., Silvola, J., and Martikainen, P. J.: Short-term effects of changing water table on N_2O fluxes from peat monoliths from natural and drained boreal peatlands. Glob. Change Biol., 5, 183-189, 1999.
Rice, S. and Giles, L.: The influence of water content and leaf anatomy on carbon isotope discrimination and photosynthesis in Sphagnum. Plant Cell Environ., 19, 118-124, 1996.
Reimer, P. J., Brown T. A., Reimer, R. W.: Discussion: Reporting and Calibration of Post-Bomb ^{14}C Data. Oak Ridge, Tennessee, U.S.A. http://dx.doi.org/10.3334/CDIAC/spruce.005, 2004.
Reimer, P. J., Bard, E., Bayliss, A., Beck, J. W., Blackwell, P. G., Bronk, R. C., Buck, C. E., Cheng, H., Edwards, R. L, Friedrich, M., Grootes, P. M., Guilderson, T. P., Haflidason, H., Hajdas, I., Hatté, C., Heaton, T. J., Hoffmann, D. L., Hogg, A. G., Hughen, K. A., Kaiser, K. F., Kromer, B., Manning, S. W., Niu, M., Reimer, R. W., Richards, D. A., Scott, E. M., Southon, J. R., Staff, R. A., Turney, C. S. M., and van der Plicht, J.: IntCal13 and Marine13 Radiocarbon Age Calibration Curves 0–50,000 Years cal BP. Radiocarbon, 55, doi:10.2458/azu_js_rc.55.16947, 2013.
Sebestyen, S. D., Dorrance, C., Olson, D. M., Verry, E. S., Kolka, R. K., Elling, A. E., Kyllander, R.: Long-term monitoring sites and trends at the Marcell Experimental Forest. In: Kolka, Randall K.; Sebestyen, Stephen D.; Verry, Elon S.; Brooks,Kenneth N., eds. Peatland biogeochemistry and watershed hydrology at the Marcell Experimental Forest. Boca Raton, FL, CRC Press, 15-71, 2011.
Skrzypek, G., Jędrysek, M., and Keller-Sikora A.: Calibration of temperature carbon isotopic effect (peat bogs Hala Izerska, Izerskie Mts. and Szrenica, Karkonosze Mts.). Pol. Geological Inst. Spec. Papers, 16, 123-126, 2005.

© Author(s) 2016. CC-BY 3.0 License.

Skrzypek, G., Paul, D., and Wojtun, B.: Stable isotope composition of plants and peat from Arctic mire and geothermal area in Iceland. Pol. Polar Res., 29, 365-376, 2008.

Sparks, J. and Ehleringer, J. R.: Leaf carbon isotope discrimination and nitrogen content for riparian trees along elevational transects. Oecologia, 109, 362-367, 1997.

Stewart, G. R., Schmidt, S., Handley, L. L., Turnbull, M. H., Erskine, P. D., and Joly, C. A.: ^{15}N natural abundance of vascular rainforest epiphytes: implications for nitrogen source and acquisition. Plant Cell Environ., 18, 85-90, 1995.

Templer, P. H., Arthur, M. A., Lovett, G. M., and Weathers, K. C.: Plant and soil natural abundance $\delta^{15}N$: indicators of relative rates of nitrogen cycling in temperate forest ecosystems. Oecologia, 153, 399-406, doi:10.1007/s00442-007-0746-7, 2007.

Tfaily, M. M., Cooper, W. T., Kostka, J., Chanton, P. R., Schadt, C. W., Hanson, P. J., Iversen, C. M., and Chanton, J.P.: Organic matter transformation in the peat column at Marcell Experimental Forest: humification and vertical stratification. J. Geophys. Res. Biogeosci., 119, 661-675, 2014.

Trudell, S. A, Rygiewicz, P. T., and Edmonds, R. L.: Patterns of nitrogen and carbon stable isotope ratios in macrofungi, plants and soils in two old-growth conifer forests. New Phytol., 164, 317-335, 2004.

Urban N. R. and Eisenreich, S. J.: Nitrogen cycling in a forested Minnesota bog. Can. J. Bot., 66, 435-449, doi:10.1139/b88-069, 1988.

Vitt, D. H.: Functional characteristics and indicators of boreal peatlands, In: R.K. Wieder and D.H. Vitt (Eds), Boreal Peatland Ecosystems, Ecological Studies, 188, Springer, Berlin, 9-24, 2006.

Verry, E. S. and Janssens, J.: Geology,vegetation, and hydrology of the S2 bog at the MEF: 12,000 years in northern Minnesota. In: Kolka, Randall K.; Sebestyen, Stephen D.; Verry, Elon S.; Brooks, Kenneth N., eds. Peatland biogeochemistry and watershed hydrology at the Marcell Experimental Forest. Boca Raton, FL, CRC Press, 15-71, 2011.

Vitt, D. H. and Wieder, R. K..: Boreal peatland ecosystems: our carbon heritage. Boreal Peatland and Ecosystems, Springer, Berlin, 425-429, 2006.

Vitt, D. H., Wieder, R. K., Scott, K. D., and Faller, S.: Decomposition and peat accumulation in rich fens of boreal Alberta, Canada. Ecosystems, 12, 360-373, 2009.

Wallander, H., Goransson, H., and Rosengren, U.: Production, standing biomass and natural abundance of ^{15}N and ^{13}C in ectomycorrhizal mycelia collected at different soil depths in two forest types. Oecologia, 139, 89-97, 2004.

Wray, H. E. and Bayley, S. E.: Denitrification rates in marsh fringes and fens in two boreal peatlands in Alberta, Canada. Wetlands, 27, 1036-1045, 2007.

Yavitt, J. B., Lang, G. E., and Wieder, R. K.: Control of carbon mineralization to CH_4 and CO_2 in anaerobic, *Sphagnum*-derived peat from Big Run Bog, West Virginia. Biogeochemistry, 4, 141-157, 1987.

Biogeosciences Discuss., doi:10.5194/bg-2016-261, 2016
Manuscript under review for journal Biogeosciences
Published: 6 September 2016
© Author(s) 2016. CC-BY 3.0 License.

11 Tables

Table 1. Peatland stages at SPRUCE based on stratigraphy at the S2 watershed in the Marcell National Forest, USA (Verry and Janssens, 2011).

Stage	Years BP	Climate
	9300-7400	4-5°C, 700 mm MAT 700
	9200-6500	Warm and dry
Rich fen-sedge peat	8400-5500	
	7400-6100	4°C →2°C, MAP 700-800 mm
	6500-6000	Cooling trend
	6100-3200	Stable climate
Transitional fen	5600-3000	
	3200-2400	Cooled slightly
Open poor fen	2900-390	
	2000-1800	Warmer and drier
Little Ice Age	600-150	Cooled 1°C, MAT 800 mm
Forested bog	384/130-now	

Table 2. Average foliar values for $\delta^{13}C$, $\delta^{15}N$, %C, %N, and C/N (n = 7). [1]Weighted average of $\delta^{13}C$ inputs is -29.2‰., based on carbon fixation measurements of different taxa (R.J. Norby, personal communication). ANOVA comparing means in vascular plants used a post-hoc Tukey test, with log C/N tested in place of C/N. [2]Data from Tfaily et al. (2014). [3]Top 10 cm only, primarily *Sphagnum*.

Species	$\delta^{13}C$±se	$\delta^{15}N$±se	%C±se	%N±se	C/N±se	n	% C flux[1]
Chamaedaphne	-29.5±0.1^{c}	-3.8±0.4^{c}	51.30±0.42^{a}	1.50±0.04^{b}	34.53±0.88^{cd}	12	1.5
Eriophorum	-28.4±0.2^{a}	2.5±0.6^{a}	45.16±0.21^{c}	1.45±0.06^{b}	31.49±1.36^{d}	9	--
Larix	-30.4±0.1^{d}	-6.3±0.4^{d}	48.49±0.36^{bc}	0.77±0.06^{c}	65.10±5.17^{b}	7	37.0
Ledum	-29.2±0.1^{bc}	-5.4±0.2^{d}	51.74±0.23^{a}	1.26±0.03^{b}	41.21±1.07^{c}	13	6.6
Picea	-28.0±0.2^{a}	-8.5±0.2^{e}	49.07±0.20^{b}	0.63±0.02^{c}	79.44±3.24^{a}	11	38.3
Smilacina	-28.7±0.2^{ab}	0.1±0.3^{b}	47.20±0.53^{d}	2.46±0.10^{a}	19.53±0.88^{e}	12	1.5
[2]*Sphagnum*	-29.2	-2.0	--	--	--	--	15.0
Hollow[3]	-28.8±0.1	-2.3±0.2					
Hummock[3]	-28.8±0.1	-2.3±0.5					

Biogeosciences Discuss., doi:10.5194/bg-2016-261, 2016
Manuscript under review for journal Biogeosciences
Published: 6 September 2016
© Author(s) 2016. CC-BY 3.0 License.

Table 3. Regression model for explaining $\delta^{13}C$ and $\delta^{15}N$ in peat profiles at SPRUCE. *Treed* vs non-treed, *hummock* vs. hollow topography. Plot and depth treated as nominal variables. Value = Coefficient ± standard error; Var. = % variance explained. n = 238. Complete regression model including values for specific plots and depths are given in Appendix 1.

$\delta^{13}C$ model, adjusted r^2 = 0.853, p <0.001				$\delta^{15}N$ model, adjusted r^2 = 0.701, p <0.001			
Source	Value±se	%Var.	P	Source	Value±se	%Var.	P
Intercept	-27.80±0.38	--	--	Intercept	25.21±4.09	--	--
$\delta^{15}N$	0.177±0.029	11.4	**<0.001**	$\delta^{13}C$	0.882±0.145	13.9	**<0.001**
%N	1.14±0.18	12.1	**<0.001**	%N	-2.566±0.406	14.9	**<0.001**
%C	-0.036±0.011	3.1	**0.002**	%C	0.089±0.025	4.8	**<0.001**
C/N	0.023±0.004	11.5	**<0.001**	C/N	-0.044±0.009	9.7	**<0.001**
Treed	-0.15±0.06	1.9	**0.014**	Treed	0.29±0.13	1.8	**0.029**
Hummock	0.32±0.12	2.3	**0.007**	Hummock	0.71±0.27	2.7	**0.008**
Plot	--	10.0	**0.008**	Plot	--	14.6	**0.001**
Depth	--	47.6	**<0.001**	Depth	--	37.5	**<0.001**

Table 4. Correlations between radiocarbon and stable isotopes by depth, and mean $\Delta^{14}C$ for that depth. Hummock vs hollow plots and treed vs non-treed plots were averaged together. $\delta^{13}C$±se and $\delta^{15}N$±se columns reflect the shift in $\Delta^{14}C$ with a 1‰ shift in $\delta^{13}C$ or $\delta^{15}N$. Statistically significant correlations are bolded. nd = not determined.

Depth	n	Mean±se $\Delta^{14}C$ (‰)	Age (cal yr BP)	$\delta^{13}C$±se adj. r^2	(‰)	P	$\delta^{15}N$±se adj. r^2	(‰)	P
25	3	52±5	Modern	0.881	10±3	0.1572	-0.943	2±9	0.8916
22	7	29±13	Modern	0.325	69±35	0.1057	-0.195	2±11	0.889
15	16	59±5	Modern	**0.219**	**13±6**	**0.0388**	**0.221**	**7±3**	**0.038**
5	16	115±18	Modern	**0.682**	**74±13**	**<0.0001**	0.039	17±14	0.2247
-5	19	71±7	Modern	**0.352**	**33±10**	**0.0044**	**0.293**	**18±6**	**0.0098**
-15	19	126±19	Modern	-0.053	9±30	0.7619	-0.024	-16±22	0.4591
-25	20	100±23	Modern	0.018	-41±35	0.2613	**0.414**	**-62±16**	**0.0013**
-35	18	-102±34	1580±180	**0.228**	**-246±100**	**0.0261**	-0.053	-9±24	0.7045
-45	18	-182±27	1730±260	-0.041	-54±95	0.575	**0.570**	**58±12**	**0.0002**
-55	18	-203±19	nd	-0.025	-63±81	0.4474	**0.512**	**52±12**	**0.0007**
-65	18	-288±11	2800±600	**0.486**	**-100±24**	**0.0008**	**0.340**	**44±14**	**0.0065**
-85	18	-359±7	3520±90	-0.007	-23±25	0.3618	-0.049	-7±15	0.6505
-113	18	-392±6	3950±90	0.081	42±27	0.1337	0.016	-17±15	0.2756
-163	17	-486±7	6000±500	**0.713**	**68±11**	**<0.0001**	**0.537**	**-31±7**	**0.0005**
-213	3	-587±32	9200±200	-0.811	-44±136	0.801	-0.96	-11±76	0.9115
-225	11	-567±12	6775±260	-0.089	27±62	0.6771	-0.101	9±33	0.7842

Biogeosciences Discuss., doi:10.5194/bg-2016-261, 2016
Manuscript under review for journal Biogeosciences
Published: 6 September 2016
© Author(s) 2016. CC-BY 3.0 License.

12 Figures

Figure 1. Conceptual diagram of movement of carbon (C) and nitrogen (N) during peatland development from rich fen to bog. Major processes influencing isotopic composition include methane (Me) flux from surficial and deeper layers (dotted upward arrow), methanotrophy and CO_2 recapture by *Sphagnum*, vascular plant transport of methane, N uptake by vascular plants, and the sequestration of C and N over time in deeper peat. Assimilation of ^{13}C-depleted CO_2 from the Suess effect influences modern peat carbon (rightmost top box); N flux from uplands influences productivity in the lagg region, and hummock and hollow topography influences methanogenesis and methanotrophy. Climate (not shown) will influence the initial $\delta^{13}C$ of fixed carbon. By rotating the figure 90° counterclockwise, the lower boxes correspond stratigraphically to the peat profile.

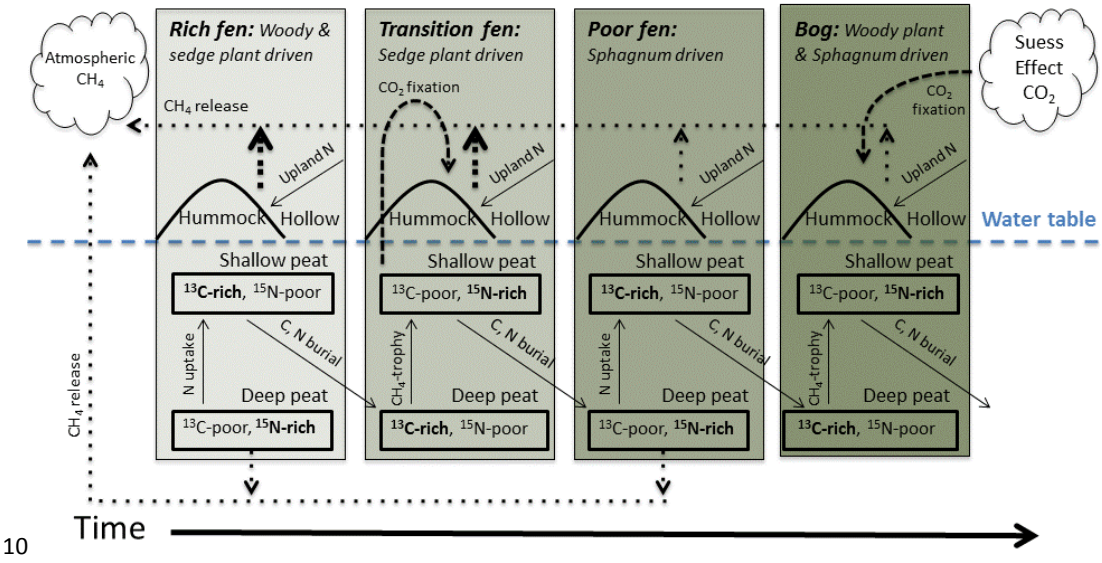

Biogeosciences Discuss., doi:10.5194/bg-2016-261, 2016
Manuscript under review for journal Biogeosciences
Published: 6 September 2016
© Author(s) 2016. CC-BY 3.0 License.

Figure 2. Aerial photograph of the S1 bog (23 September 2014) showing the 17 experimental plots (each 10.4 m in diameter to the outer edge of the visible perimeter boardwalk). Plot numbers on the image represent the plot areas within which peat was sampled.

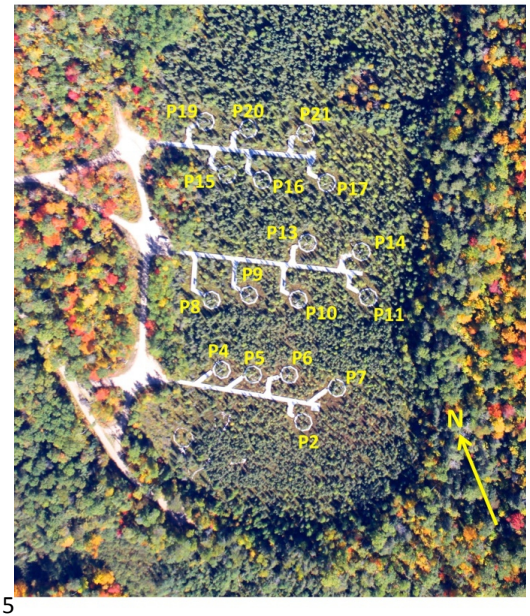

5

Biogeosciences Discuss., doi:10.5194/bg-2016-261, 2016
Manuscript under review for journal Biogeosciences
Published: 6 September 2016
© Author(s) 2016. CC-BY 3.0 License.

Figure 3. $\delta^{15}N$, $\delta^{13}C$, %N, %C, and natural log of C/N versus depth. Values (±se) are averaged across hummock versus hollow cores and across treed versus non-treed cores. Averages (±se) are given for each depth, with *n* given in parentheses following the depth: 25 cm (3), 22 cm (7), 15 cm (14), 5 cm (14), -5 cm (19), -15 cm (17), -25 cm (17), -35 cm (15), -45 cm (17), -55 cm (17), -65 cm (17), -85 cm (18), -112 cm (17), -162 cm (17), -213 cm (3), -225 cm (8).

a. $\delta^{13}C$ versus depth

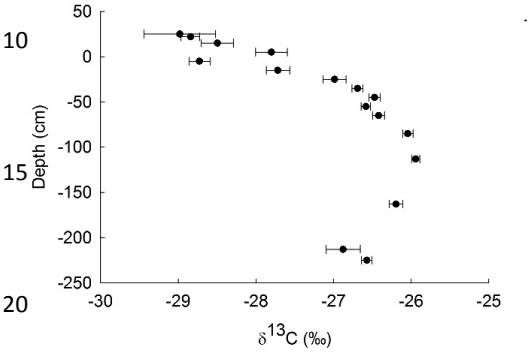

b. $\delta^{15}N$ versus depth

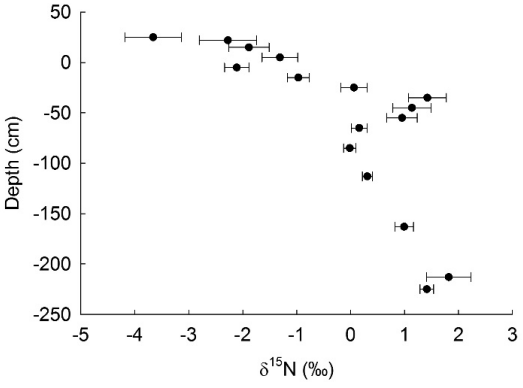

c. %C versus depth

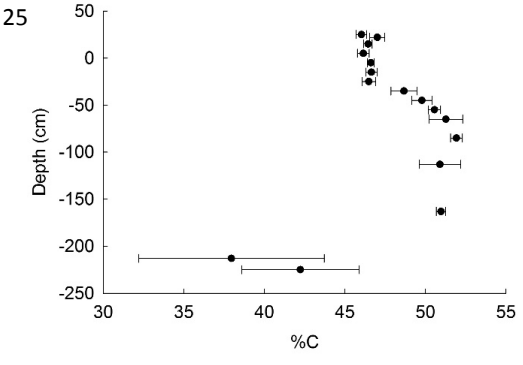

d. %N versus depth

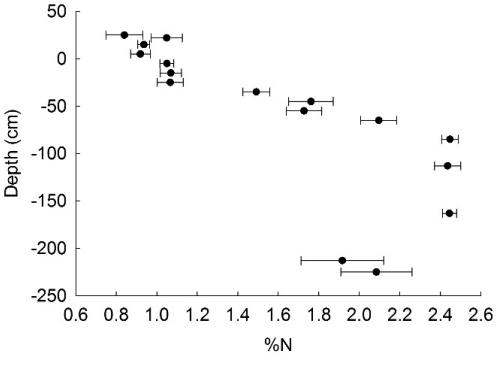

e. C/N.

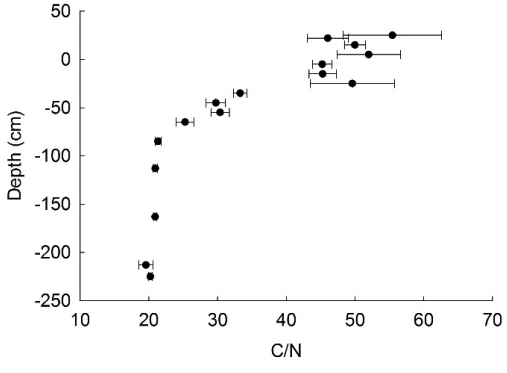

Biogeosciences Discuss., doi:10.5194/bg-2016-261, 2016
Manuscript under review for journal Biogeosciences
Published: 6 September 2016
© Author(s) 2016. CC-BY 3.0 License.

Figure 4. Depth coefficients of $\delta^{15}N$ and $\delta^{13}C$ from regression models correlate in peat profiles. The depth in cm is indicated next to coefficients (±se).
$\delta^{15}N = 1.97\pm0.44 \times \delta^{13}C + 0.00\pm0.34$, adjusted $r^2 = 0.557$, n = 16, p = 0.0005

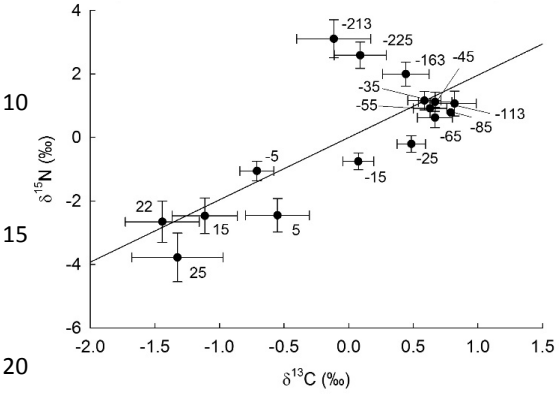

Figure 5. a. Plot coefficients of $\delta^{15}N$ and $\delta^{13}C$ from regression models correlate in peat profiles. Standard error bars omitted for clarity, and averaged 0.24‰ for $\delta^{15}N$ and 0.12‰ for $\delta^{13}C$. The plot number is the symbol for the paired coefficient values. Data plotted below, $\delta^{15}N = -1.36\pm0.46 \times \delta^{13}C + 0.00\pm0.08$, adjusted $r^2 = 0.271$, p = 0.0224, n = 16.

b. To show the spatial relationship among coefficient values, plot locations are as given in Figure 1, with plot 4 at lower left. Values are given × 10 for the $\delta^{15}N$ and $\delta^{13}C$ coefficients, as ($\delta^{15}N$, $\delta^{13}C$). Coefficients are color-coded based on $\delta^{15}N$ values, with blue = high $\delta^{15}N$, red = low $\delta^{15}N$, and purple intermediate $\delta^{15}N$.

a.

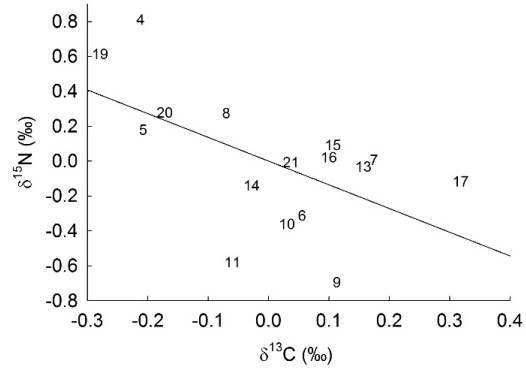

b.

-3,6	-2,3	0,0	
1,1	1,0	3,-1	
		2,0	0,-1
-1,3	1,-7	0,-4	-1,-6
-2,8	-2,2	1,-3	2,0

Biogeosciences Discuss., doi:10.5194/bg-2016-261, 2016
Manuscript under review for journal Biogeosciences
Published: 6 September 2016
© Author(s) 2016. CC-BY 3.0 License.

Figure 6. Relationship between $\Delta^{14}C$ and a) $\delta^{13}C$; b) $\delta^{15}N$.

a.

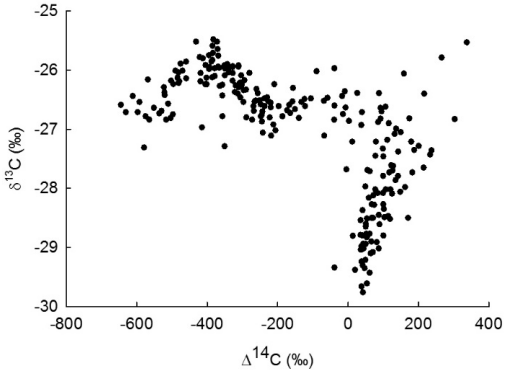

b.

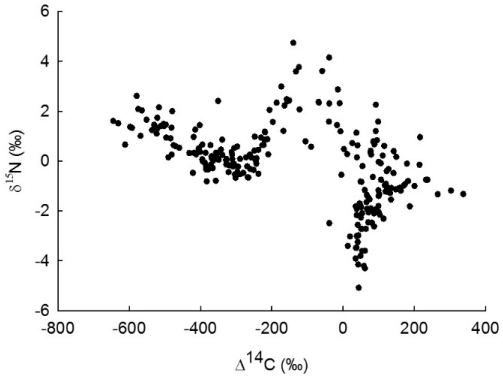

Biogeosciences Discuss., doi:10.5194/bg-2016-261, 2016
Manuscript under review for journal Biogeosciences
Published: 6 September 2016
© Author(s) 2016. CC-BY 3.0 License.

13 Appendices

Table A1. Regression model for explaining $\delta^{13}C$ and $\delta^{15}N$ in peat profiles at SPRUCE. *Treed* vs non-treed, *hummock* vs. hollow topography. Plot and depth treated as nominal variables. Value = Coefficient ± standard error; Var. = % variance explained. n = 238.

$\delta^{13}C$ model, adjusted r^2 = 0.853, p <0.001				$\delta^{15}N$ model, adjusted r^2 = 0.701, p <0.001			
Source	Value±se	%Var.	P	Source	Value±se	%Var.	P
Intercept	-27.80±0.38	--	--	Intercept	25.21±4.09	--	--
$\delta^{15}N$	0.177±0.029	11.4	**<0.001**	$\delta^{13}C$	0.882±0.145	13.9	**<0.001**
%N	1.14±0.18	12.1	**<0.001**	%N	-2.566±0.406	14.9	**<0.001**
%C	-0.036±0.011	3.1	**0.002**	%C	0.089±0.025	4.8	**<0.001**
C/N	0.023±0.004	11.5	**<0.001**	C/N	-0.044±0.009	9.7	**<0.001**
Treed	-0.15±0.06	1.9	**0.014**	Treed	0.29±0.13	1.8	**0.029**
Hummock	0.32±0.12	2.3	**0.007**	Hummock	0.71±0.27	2.7	**0.008**
Plot	--	10.0	**0.008**	Plot	--	14.6	**0.001**
Depth	--	47.6	**<0.001**	Depth	--	37.5	**<0.001**
Plot				Plot			
4	-0.22±0.09		**0.0241**	4	0.81±0.21		**0.0001**
5	-0.21±0.10		**0.0327**	5	0.18±0.22		0.4244
6	0.05±0.11		0.6733	6	-0.31±0.24		0.1933
7	0.17±0.11		0.1042	7	0.00±0.24		0.9875
8	-0.07±0.11		0.5042	8	0.27±0.24		0.2656
9	0.11±0.11		0.3187	9	-0.70±0.24		**0.0043**
10	0.03±0.11		0.8007	10	-0.36±0.24		0.1295
11	-0.06±0.11		0.5791	11	-0.58±0.25		**0.0208**
13	0.15±0.11		0.1569	13	-0.03±0.24		0.8883
14	-0.03±0.11		0.7861	14	-0.14±0.26		0.5796
15	0.10±0.12		0.3708	15	0.09±0.26		0.7274
16	0.10±0.11		0.3602	16	0.02±0.24		0.9334
17	0.32±0.11		**0.0033**	17	-0.12±0.24		0.6275
19	-0.28±0.11		**0.0088**	19	0.61±0.24		**0.011**
20	-0.17±0.11		0.1072	20	0.28±0.24		0.2562
21	0.03		--	21	-0.01		--
Depth							
25	-1.33±0.35		**0.0002**	25	-3.78±0.77		**<0.0001**
22	-1.44±0.29		**<0.0001**	22	-2.65±0.65		**<0.0001**
15	-1.11±0.25		**<0.0001**	15	-2.47±0.56		**<0.0001**
5	-0.55±0.25		**0.0266**	5	-2.45±0.53		**<0.0001**
-5	-0.71±0.13		**<0.0001**	-5	-1.06±0.31		**0.0007**
-15	0.07±0.12		0.5328	-15	-0.76±0.26		**0.0043**
-25	0.49±0.11		**<0.0001**	-25	-0.20±0.26		0.4302
-35	0.59±0.13		**<0.0001**	-35	1.16±0.29		**<0.0001**
-45	0.67±0.13		**<0.0001**	-45	1.12±0.30		**0.0002**
-55	0.63±0.13		**<0.0001**	-55	0.92±0.30		**0.0024**
-65	0.67±0.14		**<0.0001**	-65	0.63±0.32		0.0502
-85	0.79±0.16		**<0.0001**	-85	0.79±0.38		**0.0402**
-113	0.82±0.17		**<0.0001**	-113	1.07±0.39		**0.0068**
-163	0.44±0.18		**0.0145**	-163	2.00±0.38		**<0.0001**
-225	0.09±0.20		0.6549	-225	2.59±0.41		**<0.0001**
-213	-0.11		--	-213	3.11		--

Biogeosciences Discuss., doi:10.5194/bg-2016-261, 2016
Manuscript under review for journal Biogeosciences
Published: 6 September 2016
© Author(s) 2016. CC-BY 3.0 License.

Table A2. Multiple regression of sample C/N as affected by the presence of trees, topography (hummock or hollow), plot #, depth, or lab notes. Lab notes indicated whether mineral material, woody debris, or other unusual material was present. Adjusted r^2 is 0.632, n = 238, $p < 0.0001$. Depth (in cm) corresponds to that used in regression analyses of $\delta^{15}N$ and $\delta^{13}C$ in Appendix 1. Depths are indicated in centimeters.

Source	%Variance	Sum of Squares	P
Vegetation	0.04	11	0.7309
Topography	1.48	374	**0.0453**
Lab notes (4)	12.89	3247	**<0.0001**
Plot (15)	10.62	2676	**0.0217**
Depth (15)	74.96	18885	**<0.0001**

Parameter Estimates			Parameter Estimates (continued)		
Term	Estimate±se	Prob>|t|	Term	Estimate±se	Prob>|t|
Intercept	36.17±3.27	**<0.0001**	Depth [25]	30.12±6.73	**<0.0001**
Trees[no trees]	-0.49±1.41	0.7309	Depth [22]	19.83±5.39	**0.0003**
Topography[Hollow]	5.37±2.67	**0.0453**	Depth [15]	19.76±4.63	**<0.0001**
Lab Notes					
[Large root]	-5.21±8.51	0.5416	Depth [5]	23.45±4.69	**<0.0001**
[Mineral matter]	-4.19±4.91	0.3935	Depth [-5]	8.01±2.51	**0.0016**
[Mineral soil]	-6.10±6.29	0.3332	Depth [-15]	6.82±2.50	**0.007**
[normal]	-4.19±2.97	0.1604	Depth [-25]	9.15±2.41	**0.0002**
(Woody debris)	19.69	--	Depth [-35]	-4.45±2.67	0.0971
Plot[4]	-1.94±2.21	0.3815	Depth [-45]	-8.00±2.67	**0.0031**
Plot[5]	1.80±2.33	0.4404	Depth [-55]	-7.26±2.72	**0.0081**
Plot[6]	6.04±2.51	**0.0171**	Depth [-65]	-12.37±2.69	**<0.0001**
Plot[7]	2.09±2.51	0.4055	Depth [-85]	-16.40±2.67	**<0.0001**
Plot[8]	-1.50±2.62	0.5669	Depth [-113]	-16.80±2.67	**<0.0001**
Plot[9]	3.09±2.53	0.2242	Depth [-163]	-17.05±2.72	**<0.0001**
Plot[10]	-1.84±2.55	0.4714	Depth (-213)	-16.33	--
Plot[11]	7.07±2.60	**0.0071**	Depth [-225]	-18.47±3.81	**<0.0001**
Plot[13]	-7.23±2.55	**0.0049**			
Plot[14]	-1.28±2.73	0.6398			
Plot[15]	-3.81±2.81	0.1765			
Plot[16]	-2.02±2.53	0.4251			
Plot[17]	1.23±2.51	0.6234			
Plot[19]	-2.73±2.62	0.2985			
Plot[20]	-0.86±2.60	0.7409			
Plot 21	1.90	--			

Least Squares Means Table for C/N of Categories from Lab Notes

Level	Least Squares Mean±se	Mean
Large root	30.97±10.40	46.8
Mineral matter	31.98±5.48	20.02
Mineral soil	30.07±7.53	19.55
normal	31.99±1.80	34.3555
Woody debris	55.86±4.37	69.4143

Biogeosciences Discuss., doi:10.5194/bg-2016-261, 2016
Manuscript under review for journal Biogeosciences
Published: 6 September 2016
© Author(s) 2016. CC-BY 3.0 License.

Table A3. Correlation of %N with $\delta^{15}N$ by depth. Significant P values are bolded.

Depth (cm)	%N coefficent±se	P	intercept±se	P
25	1.68±5.42	0.8089	-5.07±4.61	0.4697
522	4.21±2.48	0.1506	-6.69±2.64	0.0525
15	3.88±3.17	0.2408	-5.52±2.99	0.0859
5	3.13±1.62	0.0732	-4.19±1.52	**0.0153**
-5	4.62±1.11	**0.0006**	-6.96±1.17	**<0.0001**
-15	2.58±0.71	**0.0022**	-3.73±0.78	**0.0002**
10-25	2.73±0.66	**0.0006**	-2.84±0.73	**0.001**
-35	-1.66±1.27	0.2093	3.90±1.93	0.0598
-45	-2.45±0.53	**0.0003**	5.45±0.97	**<0.0001**
-55	-2.70±0.45	**<0.0001**	5.61±0.80	**<0.0001**
-65	-0.72±0.38	0.0719	1.68±0.80	0.052
15-85	0.02±0.70	0.9788	-0.06±1.71	0.9716
-113	-0.21±0.36	0.5716	0.82±0.89	0.3686
-163	-2.21±1.14	0.0724	6.39±2.80	**0.0373**
-213	-1.99±0.27	0.0859	5.63±0.52	0.059
-225	0.01±0.24	0.9821	1.40±0.52	**0.0237**

20